Droplet Size and Velocity Distributions of Wave-Impact Sea Spray over a Marine Vessel

S.R. Dehghani[1], G.F. Naterer, Y.S. Muzychka

Department of Mechanical Engineering, Faculty of Engineering and Applied Science,

Memorial University of Newfoundland, St. John's, NL, A1B 3X5, Canada

Abstract

The spatial distribution of droplets in a spray cloud created by wave-impact sea spray and the distribution of their sizes and velocities over a vessel deck is investigated. Wave-impact sea spray, which occurs due to striking high energy sea waves on a vessel's bow, creates numerous droplets in front of a vessel. Droplets are frequently the result of sheet and droplet breakup of sea water. The velocity-size dependence of the resultant droplets is important in the modelling of marine icing phenomena. A droplet trajectory method employs the velocity-size dependence of the droplets to find their spatial distributions in the cloud of spray over the vessel deck. Drag body forces overcome the initial velocities of the droplets so they follow the wind direction and gravitational direction. The motion of the droplets affects the shape and extent of the spray cloud in front of the vessel and over the deck. In this paper, numerical methods are developed to find the distribution of sizes and velocities of the droplets over a vessel. Results show that neither the smallest nor the largest droplets reach the maximum height. The medium-size droplets can reach the maximum height of the spray cloud. As the spray cloud travels over the deck, the droplet velocities become almost the same. Comparing the numerical results with field observations shows

[1]Corresponding author, Postdoctoral Fellow, Phone: +1 (709) 771-6216, Email: srdehghani@mun.ca

that the predicted results are consistent and have reasonable agreement with the field measurements.

Keywords: Droplet size distribution, Droplet velocity distribution, Marine icing, Wave-impact sea spray, Droplet trajectory

1. Introduction

Wave-impact sea spray, which results from high energy sea waves striking a vessel bow or hull, is the main reason for marine icing in cold regions (Zakrzewski, 1987; Lozowski et al., 2000; Panov, 1978). Every spray cloud carries numerous droplets towards the vessel platform (Zakrzewski, 1986; Zakrzewski and Lozowski, 1988). The nature of the spray cloud and droplets affects the progress of ice accretion on a marine vessel (Ryerson, 1995; Borisenkov et al., 1975). A spray cloud can be defined based on time dependent spatial distributions of sizes and velocities of the droplets. The spatial distributions, including the velocity and size of the droplets, determine the spray cloud (Zakrzewski and Lozowski, 1988; Dehghani et al., 2016a).

Apart from the ambient temperature, relative humidity and wind velocity, the incoming water flux to a vessel deck is important for calculating the amount of accumulated ice on the vessel (Kulyakhtin and Tsarau, 2014; Horjen, 2013). The accumulated ice is brine-spongy ice (Dehghani et al., 2016b). The water flux varies with position and time. Size and velocity distributions of the droplets in a spray cloud determine the local spray flux at every point of a vessel. Distributions of size and velocity will yield the water flux, which will also be a function of time and space (Dehghani et al., 2016a).

Past studies reported mono-size models where there is no distribution of size and velocity for a cloud of spray (Kulyakhtin and Tsarau, 2014). Horjen (2013) used a size of 1.8 mm for the droplets. Shipilova et al. (2012) assumed 0.25 mm and 2 mm as the droplet sizes. Horjen (2015) considered the size of the droplets as 3.8 mm. Chung and Lozowski (1998) assumed the same size of droplets as Zakrzewski (1986), 1.75 mm. Kulyakhtin and Tsarau (2014) mentioned that droplet sizes are between 1 and 2 mm. These past studies assumed the initial velocity of the droplets as equal to the wind velocity. A lack of distribution of size and velocity in a spray cloud led the researchers to use mono-size and mono-velocity models.

Droplet trajectory modes can predict the droplet paths and consequently their positions. When a spray cloud moves, droplets start their movements at their initial positions and finish by impinging on vessel surfaces (Dehghani et al., 2009; Zakrzewski and Lozowski, 1988). The droplet trajectory method, which needs the initial size and velocity distributions, will determine the distribution of the size and velocity of the droplets at every section of the spray cloud, and consequently, the final distribution of the spray flux over the vessel surfaces (Dehghani et al., 2013; Dehghani et al., 2016a).

The liquid water content (LWC) of a spray cloud over a vessel deck ise affected by the distributions of size and velocity of droplets over a vessel platform (Ryerson, 1995; Dehghani et al., 2016a). The collision efficiency, which is a key parameter in calculating the fraction of impingement of the droplets on a specific surface, is also a function of the size and velocity of the droplets close to the surface (Zakrzewski, 1986). The freezing rate can be affected by the incoming flux of water and the collision efficiency. Both are also dependent on the distribution of size and velocity of droplets (Chung et al., 1998a; Chung et al., 1998b; Sharpov, 1971; Shipilova, et al. 2012).

Therefore, determination of the distributions of size and velocity of the droplets and their variations over marine vessels during the motion of a spray cloud are essential for accurate modelling of marine icing phenomena (Zakrzewski and Lozowski, 1988). The assumptions of constant droplet sizes and velocities used in previous models of marine icing are not satisfactory. This assumption does not yield a sufficiently accurate estimation of ice accretion over a marine vessel. A vertically uniform size and velocity are the most common assumption in past studies (Horjen, 2013; Horjen, 2015; Kulyakhtin and Tsarau, 2014; Lozowski et al., 2000; Shipilova, et al., 2012).

This paper focuses on new models for the distributions of size and velocity of droplets in a spray cloud over a marine vessel, using a droplet trajectory method and droplet-size-dependent characteristics after water breakup in front of a vessel. A new distribution of size and velocity is presented. The distribution of size and velocity can determine the extent of the spray cloud over a vessel. The model will be examined and compared against data from field observations.

2. Spray Cloud Processes

Wave-impact sea spray is created by high energy sea waves striking a vessel bow or hull (Dehghani et al., 2016a; Zakrzewski, 1986). The process of creating a spray cloud and its development and motion can be divided into several stages: wave impact, sheet breakup, droplet breakup, spray cloud formation, spray cloud acceleration and deceleration, and spray cloud fall and impingement. These stages have not been well understood (Dehghani et al., 2016a; Ryerson 1995). The mechanism of sheet creation, sheet breakup and droplet breakup have been examined in a few past studies but need more investigation (Bullock et al., 2007; Galiev and Flay, 2014; Greco et al., 2013; Gu et al., 2014; Ren and Marshall, 2014; Dehghani et al., 2016a).

After the stage of droplet breakup, there are numerous droplets with various sizes and velocities in the spray cloud. At the front edge of the vessel, the droplets are moving upward and in the same direction as the vessel. The stage of spray cloud formation begins with decelerating and accelerating droplets. Upward movement of the droplets is decelerated by drag forces and body forces. Drag forces are created as a result of the relative velocity of the droplets and wind. Body forces occur with the gravity force exerted on the droplets. Due to the drag force and body force, the vertical component of droplet velocities decreases to reach zero. At this point, droplets reach their maximum height. The horizontal components of the droplet velocities experience the same trend. The start of the horizontal movement of the droplets is usually in the opposite direction of the wind velocity. The wind slows down the droplets. After a short period, in the decelerating period, the horizontal velocities of the droplets become zero. This point is the maximum horizontal development of a spray cloud in the opposite direction of the wind.

Droplets with a vertical velocity of zero, which are at their maximum heights, start downward movement because of gravity. This accelerates the droplets to reach their terminal velocities. The droplets with zero horizontal velocities are affected by the wind velocity and increase their velocities. The wind accelerates these droplets and increases their velocities to the wind velocity. Accelerating the droplets is continued until the droplets impinge on the vessel surfaces.

The spray cloud fall and droplet impingement are the last stages of motion of a spray cloud over a marine vessel. The various droplets with various sizes and velocities take different paths and reach different positions. The drag force, wind velocity, droplet size, and initial velocity of droplets determine the trajectory of the droplets. Figure 1 illustrates these stages of a spray cloud development related to wave-impact sea spray over a marine vessel. The vessel chosen is the same as a Medium-size Fishing Vessel (MFV) (Borizenkov et al., 1975; Zakrzewski, 1986; Sharpov, 1971). The important components of the MFV are illustrated in the figure. The overall length of the vessel is about 39.5 m. The foremast is located at 11.0 m from the ship bow. The front side of the structure is located at a distance of 19.2 from the ship bow. The height of the structure above the deck is 4.5 m. The life boat is located 29.0 to 34.1 m from the ship bow (Zakrzewski and Lozowski, 1988).

The initial velocities and sizes of droplets at the front edge of a marine vessel are among the most essential elements for predicting the droplet trajectories. A velocity-size dependence suggests that after the droplet breakup stage, the larger droplets have lower velocities and the smaller droplets have higher velocities. This means at the front edge of the vessel, there is a velocity-size dependence for the droplets that can be used for the initial conditions. Dehghani et al. (2016a) reported this velocity-size dependence.

3. Formulation of Spray Cloud Motion

Spherical droplets, having a density of ρ_d and a diameter of D_d, are small compared to the flow length scale (the bow dimension). Applying Newton's Second Law for the droplet motion and substituting the body force and drag force will result in the following equation of the droplet trajectory. The equation describing to droplet movement and the forces acting on them can be expressed as:

$$m_d \frac{d\boldsymbol{V_d}}{dt} = \rho_d \forall_d \mathbf{g} - C_{dr} \frac{\pi D_d^2}{8} \rho_a |\boldsymbol{V_d} - \boldsymbol{V_a}|(\boldsymbol{V_d} - \boldsymbol{V_a}) + \rho_a \forall_d C_{ad} \frac{D(\boldsymbol{V_a} - \boldsymbol{V_d})}{Dt} + \rho_a \forall_d \left(\frac{D\boldsymbol{V_a}}{Dt} - \mathbf{g}\right) \quad (1)$$

where m_d is mass of the droplet, t is time, $\boldsymbol{V_d}$ is droplet velocity, $\boldsymbol{V_a}$ is air velocity, ρ_d is water density, $\forall_d$ is droplet volume, $\mathbf{g}$ is gravity, C_{dr} is drag coefficient, D_d is droplet diameter, ρ_a is air density, and C_{ad} is added mass force coefficient. The coefficient C_{ad} is assumed to be 0.5 and C_{dr} can be calculated as follows (Dehghani et al. 2009):

$$C_{dr} = \begin{cases} \frac{24}{Re} & Re < 1 \\ \frac{24}{Re}\ (1 + 0.15Re^{0.687}) & 1 < Re < 1000 \\ 0.44 & Re > 1000 \end{cases} \tag{2}$$

In order to solve this equation, its unknowns are calculated separately. Substituting the unknowns leads to a set of ordinary differential equations as follows.

$$\dot{x} = \frac{dx}{dt}, \qquad \ddot{x} = \frac{d^2x}{dt^2}, \qquad \ddot{x} = -\frac{3C_{dr}}{4D(\gamma + C_{ad})}(\dot{x} - U)\sqrt{(\dot{x} - U)^2 + \dot{z}^2} \tag{3}$$

$$\dot{z} = \frac{dz}{dt}, \qquad \ddot{z} = \frac{d^2z}{dt^2}, \qquad \ddot{z} = \left(\frac{1-\gamma}{\gamma + C_{ad}}\right)\mathrm{g} - \frac{3C_{dr}}{4D(\gamma + C_{ad})}(\dot{z})\sqrt{(\dot{x} - U)^2 + \dot{z}^2} \tag{4}$$

where $x, \dot{x}$, $\ddot{x}$, $z, \dot{z}$, and $\ddot{z}$, are position, velocity, and acceleration of the droplets, γ is the liquid density to air density ratio, and U is the relative velocity of wind to the vessel. The initial conditions are droplet sizes and velocities. This set of six equations and six unknowns is solved with a standard numerical solver.

There are various suggested formulae for LWC due to wave-impact sea spray, but many are intended for offshore structurers (Forest et al., 2005). The field observations of Borisenkov et al. (1975) are the most relevant data that can be used in this instance. These data related to the MFV which are suitable for our model and can be used to examine the droplet trajectory results. The proposed relation that represents the liquid water content is given by:

$$w = 24.2 \times \exp(-0.55z) \qquad gr_{water}/m^3{}_{air} \tag{5}$$

where z is the elevation above the deck of the MFV (Zakrzewski, 1987) and w is the LWC.

4. Numerical Results

The spray cloud motion can be quantified using the previous droplet trajectory model. Initial sizes of the droplets are chosen based on past work by Ryerson (1995), who reported the droplet sizes in a range from close to zero to 7.7 mm. Therefore, the initial distribution of sizes contains droplet diameters from zero to 7 mm. The initial velocity distribution is chosen by considering the velocity-size dependence of the droplets at the end of water breakup. In this case, the maximum initial velocity is considered as 60 m/s. Therefore, there is a distribution of size and velocity that can be used as the initial condition at the front edge of the vessel. The model assumes that the wind velocity is uniform, horizontal and equal to 11 m/s, which is equal to the wind velocity of the MFV on the Sea of Japan as reported by Borisenkov et al. (1975). The heading angle is considered as 180º. The ship velocity is assumed to be 2.83 m/s, which is equal to the MFV velocity on the Sea of Japan as reported by Borisenkov et al. (1975). The mass fraction of evaporation is assumed negligible. The spray is assumed dilute; therefore, the droplets will not affect each other and the droplet trajectory can be used for every droplet individually. The breakup is assumed to be finished at the vessel edge in front of the vessel.

The extent of the spray cloud is the first important parameter in the marine icing analysis. A high spray cloud can cause the creation of ice on the high elevations of the vessel. The accumulated ice on the high elevations changes the center of mass of the vessel to a higher level. This phenomenon causes an instability of the vessel that increases the risk of capsize. Therefore, the height of spray is an important factor in the modelling of marine icing phenomena. Figure 2 shows the results of the numerical solution, which are attached to the vessel sketch. The droplet trajectory method results in the creation of droplet paths over the deck. The dashed lines represent droplet paths over the vessel deck. The model calculates a full distribution of sizes and velocities as mentioned before. Figure 2 shows the trajectories of some droplets to represent the spray cloud. The spray cloud impinges on the foremast and the front side of the structure. Therefore ice accretion on these surfaces is expected. The spray cloud cannot reach the roof of the structure and the other areas that are far from the front of the vessel.

The largest and smallest droplets cannot reach the highest positions. Figure 2 shows that 6.6 mm droplets fall to the deck very quickly. Their maximum heights are less than 0.2 m and their maximum ranges are less than 0.6 m. The maximum height for the droplets with a 0.3 mm diameter is about 1.5 m. The maximum height occurs for the medium-sized droplets. The droplets with 2.4 to 3.8 mm diameter can reach the maximum height which is about 8 m and is located between the front edge of the vessel and the foremast.

The smaller droplets are rapidly affected by the wind. They are light and the wind can carry them more easily than heavy droplets. A competition between drag forces and the body forces determines the paths of the droplets. Larger droplets are heavy and lower velocity, while smaller droplets are light and higher velocity. Higher velocity droplets imply higher drag forces. Therefore, medium-size droplets are faced with values of body and drag forces that let them travel to the maximum height. The small and large droplets cannot reach the highest height because of their drag forces and body forces respectively.

Analyzing the vertical distribution of droplet sizes can clarify the extent of motion of the spray cloud. Figure 3 shows the size distribution of the droplets in the spray cloud in five cross sections. At $x = 0$, which occurs at the front edge of the vessel, the droplet size distribution includes droplets with sizes from 7 mm to very small droplets. The maximum height in this section is about 6 m. The larger and smaller droplets are at lower heights. The medium-size droplets can reach the high heights. At $x = 5\ m$, the maximum height of the spray cloud occurs. The maximum height is about 8 m. There are no droplets larger than 6 mm in this section. This means that 6 to 7 mm droplets fall to the deck between $x = 0$ and $x = 5\ m$. The next section, $x = 10\ m$, includes the droplet sizes smaller than 5.3 mm. The maximum height is less than 7 m. For the last section, the droplet sizes are limited to less than 4.6 mm. This means the larger droplets, which are heavier, fall to the deck before reaching this section. As with the other sections, the larger and smaller droplets are at lower heights and the medium-size droplets can reach higher heights.

Vertical distributions of the droplet velocities are further important factors. Figure 4 shows the vertical distribution of the horizontal component of the velocity of the droplets in the five sections. In the first section, at $x = 0$, the distribution is completely different than the other sections. This section is located at the acceleration stage and the droplets are accelerated by the wind. The droplets are at the minimum horizontal velocities. The wind velocity will affect the droplets and carry them. The horizontal velocity of the droplets is expected to increase. In the next sections, the horizontal velocity increases. Figure 4 shows that the maximum velocity will be less than 14 m/s, which is very close to the relative velocity of the vessel and wind. The small droplets will have the same velocity as the wind after the second section. The difference between the horizontal velocities in each section decreases as x increases. This means the droplets tend to reach a uniform horizontal velocity as they travel over the deck.

The vertical distributions of the vertical components of the velocities of the droplets vary as the spray cloud travels. As with the horizontal velocity, the distribution of the vertical velocities in the section of $x = 0$ is different. Droplets are decelerated to a zero velocity. In this section, the droplets move upward and the vertical velocity is positive. The maximum vertical velocity is less than 11 m/s. In the other sections, the droplets are falling. The minimum velocity is about 8.2 m/s. The differences between the vertical velocities of the droplets increase as they travel over the deck. They are affected by the forces, drag force and body force, in different ways.

The distributions of the total velocity of the droplets are shown in Figure 6. The total velocities vary between 0.4 and 14 m/s. For $x = 0$, the droplet velocities vary between 0.4 and 12.4 m/s. This is the widest range of the velocities. Some droplets, the largest, have the lowest velocity and some droplets, the smallest, have the highest velocity. The tightest range occurs for $x = 15\ m$. In this section, the velocities of the droplets are about 14 m/s. As the spray cloud travels over the deck, the differences between the velocities decreases. The droplets correct their velocities and reach almost the same velocities after a short time.

As the spray cloud travels over the deck, large and low velocity droplets fall to the deck. Therefore, the LWC is expected to decrease. Figure 7 shows the variation of the LWC over the MFV at various x distances to the front edge of the vessel. The maximum amount of LWC occurs at $x = 0$, which is at the front of the vessel. At this point the variation of the LWC vs. height is approximately exponential. At $x = 5\ m$, the height of the spray increases but LWC decreases and the curve fluctuates between 3 and 4 gr/m^3. At $x = 10\ m$, the height of the spray decreases and the LWC decreases as well. The LWC is about 1 gr/m^3 at $x = 20\ m$. This position is close to the front side of the structure of the vessel.

Droplet movements can be forward, which means co-flowing with the wind velocity, backward, which is a counter-direction with the wind velocity, upward, which is against gravity, and downward. The travel angle can define the type of movement. The angles between zero and 90° mean forward-upward directions and the angles between zero and -90° mean forward-downward directions. Figure 1 illustrates the definition of the travelling angle, θ. Figure 8 shows the distributions of the traveling angles at various sections. At $x = 0$, the droplets are moving in forward-upward directions. This means the droplets are travelling towards the vessel and also towards the higher heights. All the droplets at $x = 5\ m$ are travelling downward. This means they are in the stage of descent. As the spray cloud travels over the deck, the medium-size droplets move increasingly downward. This means the medium-size droplets are the last droplets that are affected by gravity.

Analyzing the distribution of size and velocity of the droplets can show that at the acceleration and deceleration stages, the droplets are expanding the spray cloud. After a full expansion, they start falling. The wind velocity affects the droplets in different ways. The smaller droplets are carried by wind and the larger droplets impinge on the deck rapidly.

The drag force is a key factor in analyzing the spray cloud movement. The drag force resists movement of the droplets in the air stream. The horizontal component of the drag force is a resistance force in the direction of the wind velocity. The maximum resistance occurs at the start of the development of the spray cloud when droplets are injected into the wind stream in the opposite direction. The drag force reduces the droplet velocities and decelerates them. The acceleration stage is started when droplets reach their minimum velocities. The droplets are accelerated and their velocities are increased over the deck. Figure 9 shows the distributions of the horizontal components of the drag forces of the droplets over the MFV. As the figure shows, the resistance force is higher at $x = 0$, especially for the small and high velocity droplets. This causes the droplets to reduce their velocities. At $x = 5\,m$, the drag force decreases, the droplets are accelerated, and their velocities become close to the wind velocity. At $x = 10, 15,$ and $20\,m$, the situations are the same. The droplet velocities are closer to the wind velocity and the drag forces decrease. Figure 9 shows that the horizontal drag forces occur in the same direction as the wind velocity. This means the drag force helps droplets to be aligned with the wind throughout the process of the spray cloud development.

The vertical components of the drag forces affect the vertical movements of the droplets. At the start of the spray cloud formation, the vertical drag force is downward. This reduces the droplet velocities and prevents their further upward movement. The droplet velocities reach zero and then start falling down. At $x = 0$, the drag forces are negative and in the other sections the drag forces are positive. At the start of the formation of the spray cloud, the vertical components of drag forces tend to reduce the upward velocities of the droplets. In the other sections, the droplets are falling down and the drag forces tend to resist their fall.

Figure 11 shows the distributions of the body forces in five sections over the deck of the MFV. The larger droplets have the higher body forces. The balance of the body force and the vertical component of the drag force determine the vertical movement of the droplets in the cloud of spray. The maximum body force occurs for the largest droplets, which are located at $x = 0$. As the spray cloud moves ahead, the large droplets fall down and the maximum value of the body forces reduces. Comparing Figs. 10 and 11 shows that as the spray cloud moves over the deck, the differences between the drag forces and body forces decrease. This shows that the droplets reach their terminal velocities in the last sections.

Figure 12 shows the distributions of the total drag forces in various cross-sections over the MFV. The maximum drag force occurs for the high velocity droplets at $x = 0$. These droplets that are the smallest sizes reduce their velocities in a short period. The drag force for the largest droplets is not the minimum drag in this section. The largest droplets have the smallest velocities and drag forces. The medium-size droplets that have a medium velocity and size have a moderate drag force. They are not heavy enough to be affected by gravity and they are not fast enough to be stopped by the drag force. This explains why they can reach the maximum height in the spray cloud. For the other sections, the drag forces decrease because of the lower relative velocities. The small droplets that have the same velocity as the wind have small drag forces.

The effect of the spray cloud on some parts of the MFV has been reported by Sharpov (1971). Table 1 shows a comparison between the results of the present model, observations of Sharpov (1971), and the results of Zakrazowski and Lozowski (1988). As shown in the table, the wet height of the foremast, which is the minimum height of the foremast hit by the spray cloud, is predicted as about 6.28 m. In this situation, the prediction of Zakrazowski and Lozowski (1988) is about 5.85 m and the observation of Sharpov (1971) is between 5.9 and 7.9 m. The model predicts that the front side of the structure becomes wet. The wet height is about 2.33 m. The result of Zakrazowski and Lozowski (1988) is 2.07 m and Sharpov (1971) does not mention the wet height, but mentions that the spray hits the front side of the superstructure. The spray cloud cannot wet the other parts such as the roof of the structure, the boat deck, and the safety boat. The model, predictions and the observations are in a reasonable agreement.

Figure 13 shows a comparison between the LWC measured by Borisenkov et al. (1975) and the LWC obtained by the numerical model. The numerical results are well aligned with the measured results. The exponential form of the fitted curve of the observations is in useful agreement with the numerical results. The LWC corresponds to the section of $x = 0$, which is the front edge of the vessel. The maximum height of the spray at $x = 0$ is about 6 m. Therefore the LWC varies at this height.

The model can be used to find the distribution of sizes and velocities in a cloud of wave-impact sea spray. The droplet trajectories of the droplets, by considering the drag and body forces, establish the paths and velocities of numerous droplets in the cloud of spray. The initial sizes are based on the velocity-size dependence of the droplets, which was reported by Dehghani et al. (2016a). The results of the numerical model will provide the dispersion of the droplets in front of the vessel and the way the spray cloud travels over the deck. The model can be used to determine the distributions of the sizes and velocities of the droplets in a cloud of spray. Using this model can help marine icing researchers to gain a better understanding of the incoming water flux at every point of a vessel.

5. Conclusions

Distributions of the droplet sizes and velocities were obtained by using velocity-size dependence of the droplets at the end of the breakup process and a droplet trajectory method. A vertical distribution of sizes shows that the assumption of uniform sizes for the droplets would not be accurate. The numerical results show that the smallest droplets, which are the high velocity droplets, are slowed down by drag forces rapidly. The largest droplets, which are the low velocity droplets, fall soon because of gravity. Therefore, medium-size droplets reach the highest elevations. The distribution of the vertical velocities of the droplets shows that the upward droplets change their movement to the downward direction after about 5 m traveling over the deck. The maximum velocity increases as the spray cloud moves on the vessel. The horizontal drag force is maximum at the stage of formation of the spray cloud. Drag forces change the droplet movement directions. Body forces are dominant forces in the vertical direction. The droplets are affected by the body forces and fall soon. Numerical results show that the maximum impingement height, predicted by the model, is aligned with the field observations reported by Sharpov (1971). The LWCs obtained by the numerical solutions are well aligned with the field observations reported by Borisenkov et al. (1975). The new model provides a useful method for estimating the size and velocity distribution in a cloud of spray.

Acknowledgments

The authors gratefully acknowledge the financial support from Statoil (Norway), MITACS, and Petroleum Research Newfoundland and Labrador (PRNL) for this research.

References

Borisenkov, Y.P., Zablockiy, G.A., Makshtas, A.P., Migulin, A.I., Panov, V.V., 1975. On the approximation of the spray cloud dimensions. Arkticheskii I Antarkticheskii Nauchno-Issledovatelskii Instit. Trudy Leningrad: Gidrometeoizda (in Russia), pp. 121-126.

Bullock, G.N., Obhrai, C., Peregrine, D.H., Bredmose, H., 2007. Violent breaking wave impacts. Part 1: Results from large-scale regular wave tests on vertical and sloping walls. Coastal Engineering, 54, 602-617.

Chung, K.K., Lozowski, E.P., 1998. A Three-Dimensional Time-Dependent Icing Model for a Stern Trawler. Journal of Ship research, 42(4), 266-273.

Chung, K.K., Lozowski, E.P., Zakrazewski, W.P., Gagnon, R., Thompson, T., 1998. Spraying experiments with a model stern traveler. Journal of Ship research, 42(4), 260-265.

Dehghani, S.R., Muzychka, Y.S., Naterer, G.F., 2016a. Droplet Trajectories of Wave-Impact Sea Spray on a Marine Vessel. Cold Region Science and Technology, (Accepted).

Dehghani, S.R., Naterer, G.F., Muzychka, Y.S., 2016b. Phase Change Heat Transfer in Brine-Spongy Ice. Cold Region Science and Technology, (under review).

Dehghani, S.R., Saidi, M.H., Mozafari, A.A., Ghafourian, A., 2009. Particle Trajectory in a Bidirectional Vortex Flow. Particulate Science and Technology, 27, 16–34.

Dehghani, S.R., Saidi, M.H., Mozafari, A.A., Soleimani, F., 2013. Particle Dispersion Dependency on the Entrance Position in Bidirectional Flow. Particulate Science and Technology, 31, 576–584.

Forest, T.W., Lozowski, E.P., Gagnon, R., 2005. Estimating Marine Icing on Offshore Structures using RIGICE04. IWAIS XI, Montréal, June 2005.

Galiev, S.U., Flay, R.G.J., 2014. Interaction of breaking waves with plates: The effect of hull cavitation. Ocean Engineering, 88, 27-33.

Greco, M., Colicchio, G., Lugni, C., Faltinsen, O.M., 2013. 3D domain decomposition for violent wave-ship interaction. International Journal for numerical methods in engineering, 95, 661-684.

Gu, H.B., Qiana, L., Causona, D.M., Minghama, C.G., Lin, P., 2014. Numerical simulation of water impact of solid bodies with vertical and oblique entries. Ocean Engineering. 75, 128-137.

Horjen, I., 2013 Numerical modeling of two-dimensional sea spray icing on vessel-mounted cylinders. Cold Regions Science and Technology, 93, 20–35.

Horjen, I., 2015. Offshore drilling rig ice accretion modeling including a surficial brine film. Cold Regions Science and Technology, 119, 84–110.

Kulyakhtin, A., Tsarau, A., 2014. A time-dependent model of marine icing with application of computational fluid dynamics. Cold Regions Science and Technology, 104–105, 33–44.

Lozowski, E.P., Szilder, K., Makkonen, L., 2000. Computer simulation of marine ice accretion. Philosophical Transactions of the Royal Society, London, A, 358, 2811-2845.

Panov, V.V., 1978. Icing of Ships. Polar Geography, 2 (3), 166-186.

Ren. N., Marshall, A.W., 2014. Characterizing the initial spray from large Weber number impinging jets. International Journal of Multiphase Flow, 58, 205-213.

Ryerson, C.C., 1995. Superstructure spray and ice accretion on a large U.S. Coast Guard cutter. Atmospheric Research, 36 (3–4), 321–337.

Sharpov, A.V., 1971. On the intensity of superstructure icing of small vessels (MFV type). In Theoretical and Experimental Investigations of the Conditions of Ship Icing, 95-97.

Shipilova, O., Kulyakhtin, A., Tsarau, A., Libby, B., Moslet, P.O., Loset, S., 2012. Mechanism and Dynamics of Marine Ice Accretion on Vessel Archetypes, OTC-23762-MS, OTC Arctic Technology Conference, December, Houston, Texas, USA.

Zakrzewski, W.P., 1986. ICING OF SHIPS. PART I: SPLASHING A SHIP WITH SPRAY. NOAA Technical Memorandum ERL PMEL-66.

Zakrzewski, W.P., 1987. Splashing a ship with collision-generated spray. Cold Regions Science and Technology, 14 (1), 65–83.

Zakrzewski, W.P., Lozowski, E.P., 1988. Estimating the extent of the spraying zone on a sea-going ship. Ocean Engineering, 15(5), 413–429.

Table 1. Comparison between numerical results, field observations, and previous data

Positions on the Vessel	Results		
	Zakrazowski and Lozowski (1988)	Sharpov (1971)	Numerical Results
Wet height of the foremast	5.85 m	5.5 to 7.9 m	6.28 m
Front side of the structure	2.07 m	Spray hits	2.33 m
Roof of the structure	No spray	No spray	No spray
Boat deck	No spray	No spray	No spray
Entire vessel sprayed	No	No	No

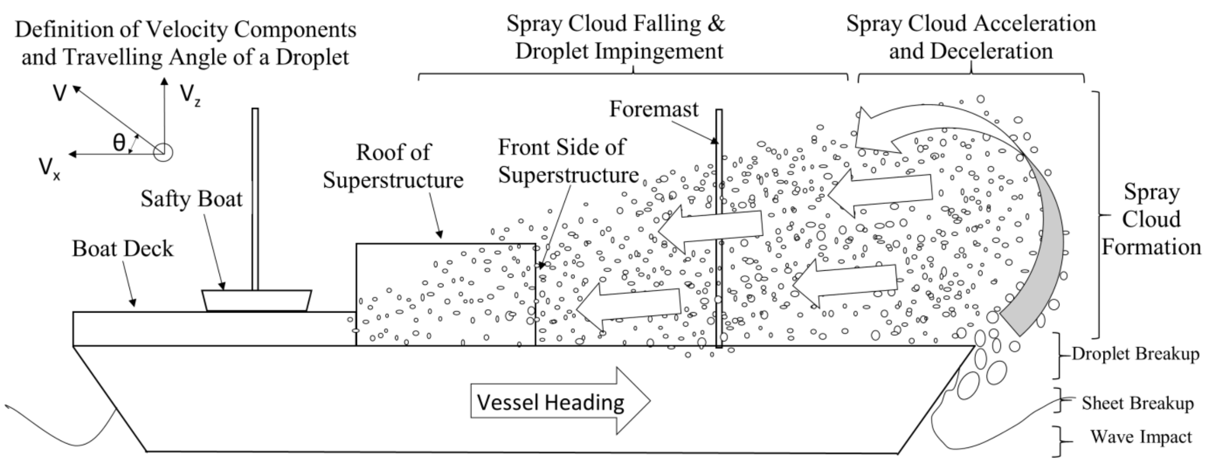

Fig. 1. Schematic of the development stages of wave-impact sea spray from creation to destination over a MFV

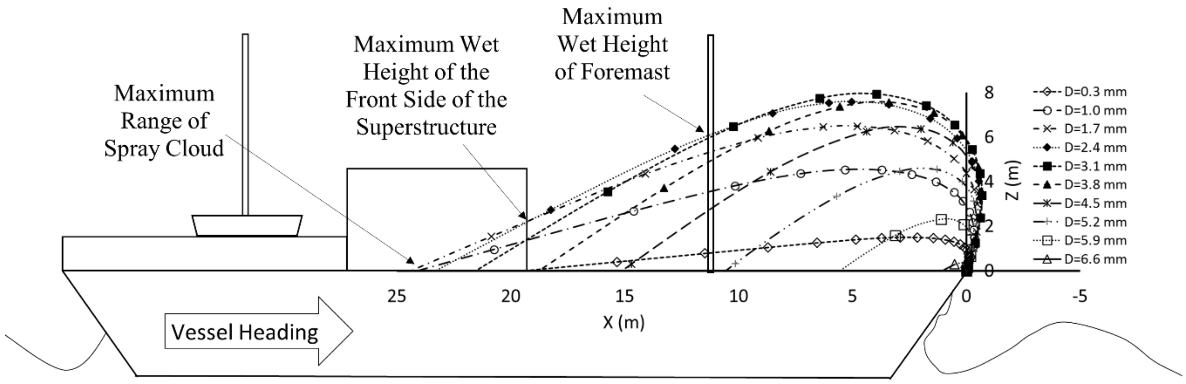

Fig. 2. Droplet trajectories of the spray cloud over the MFV and the maximum wet heights and maximum extent of the spray cloud

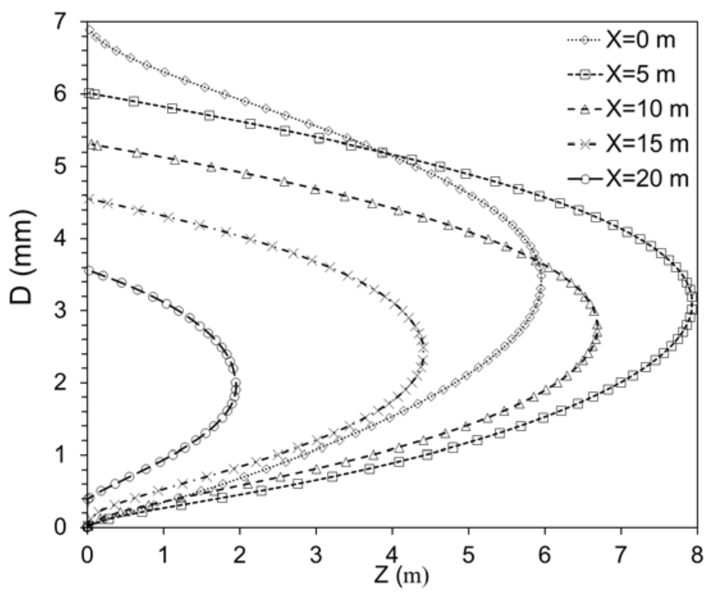

Fig. 3. Vertical distribution of the droplet sizes in a wave-impact sea spray

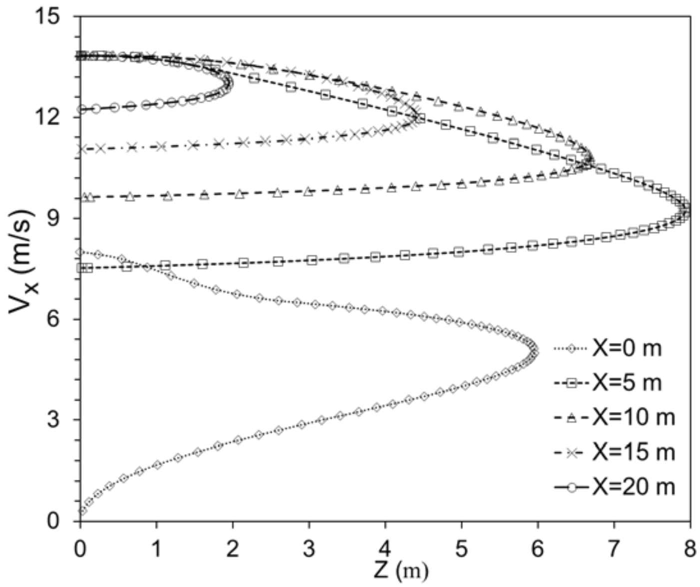

Fig. 4. Vertical distribution of the horizontal components of the droplet velocities in a spray cloud

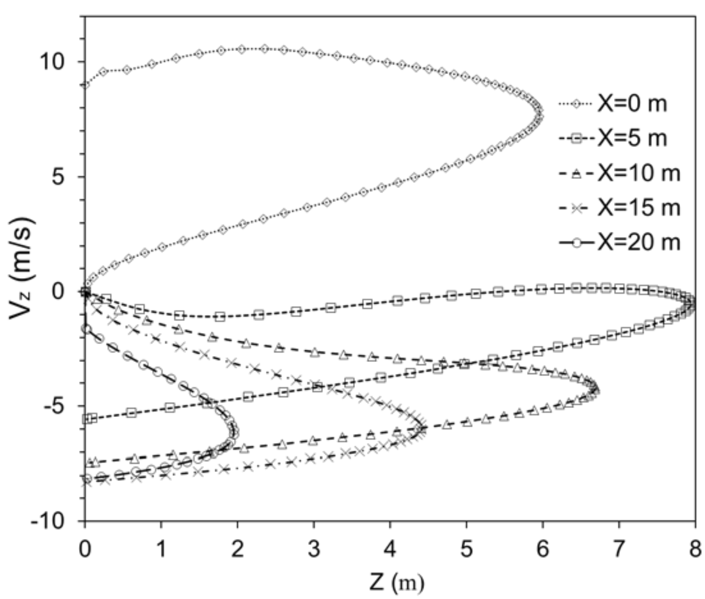

Fig. 5. Vertical distributions of the vertical components of the droplet velocities in a spray cloud

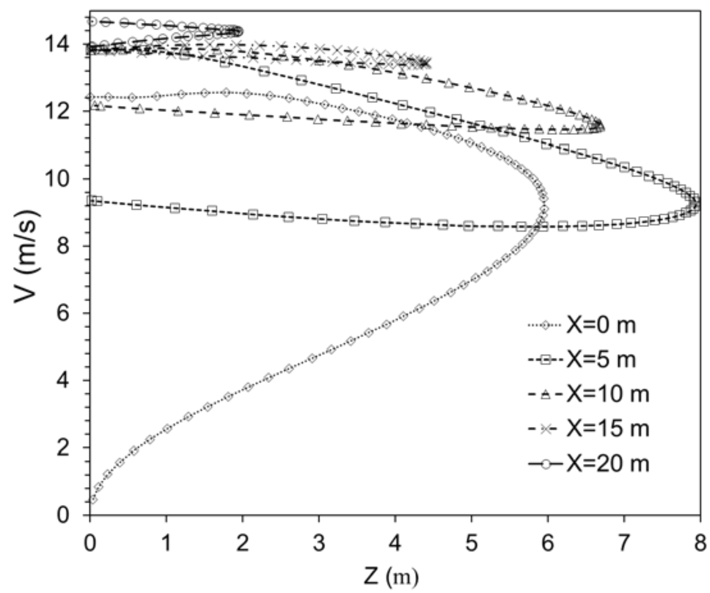

Fig. 6. Vertical distribution of the droplet velocities in a wave-impact sea spray

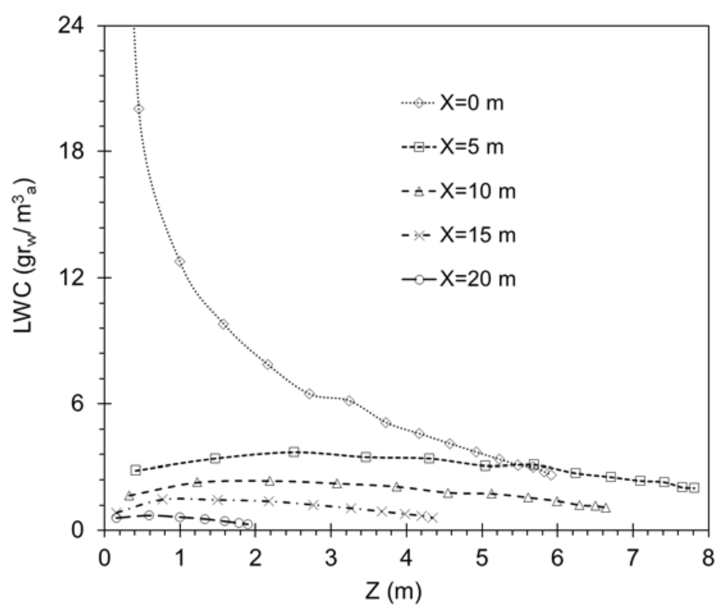

Fig. 7. Variations of the LWC at various distances from the bow

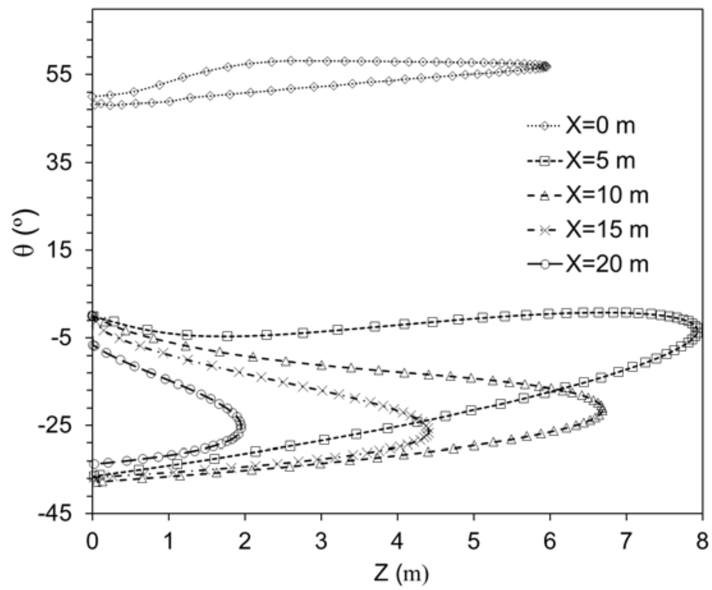

Fig. 8. Vertical distribution of the traveling angles of the droplets in a spray cloud

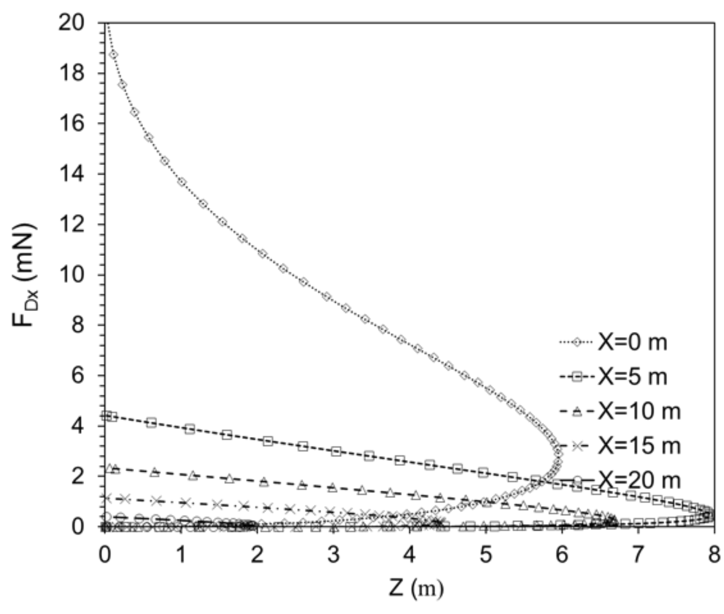

Fig. 9. Vertical distributions of the horizontal components of drag forces exerted on the droplets

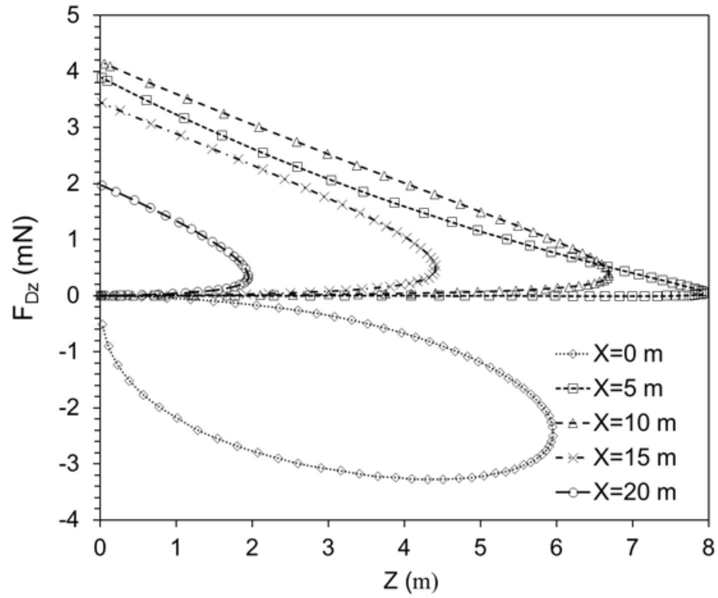

Fig. 10. Vertical distribution of vertical components of drag forces exerted on droplets

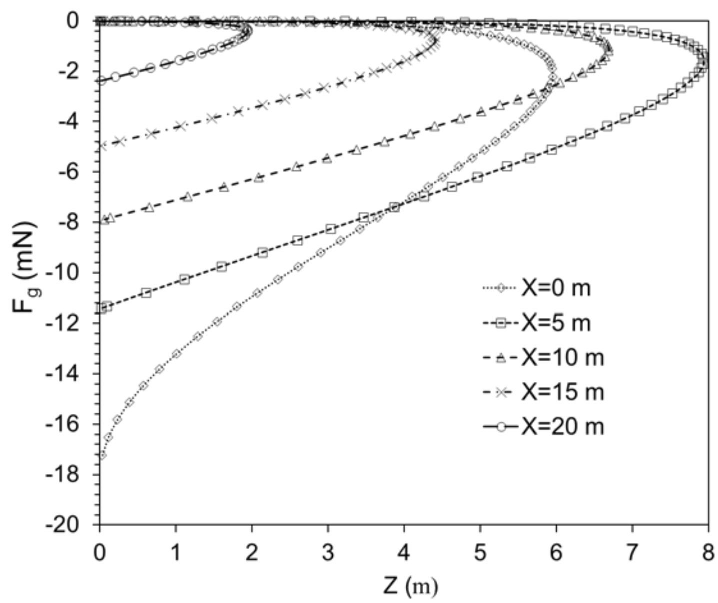

Fig. 11. Vertical distributions of the body forces of the droplets over the MFV

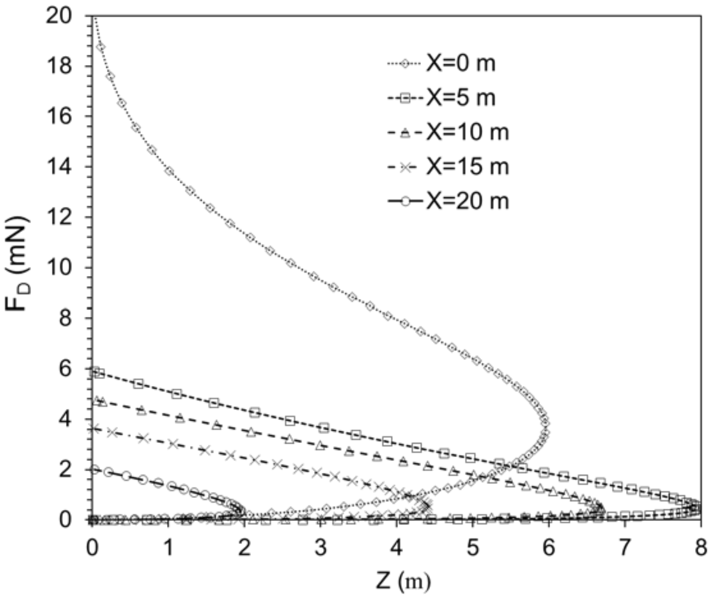

Fig. 12. Vertical distributions of total drag forces exerted on the droplets travelling on the MFV

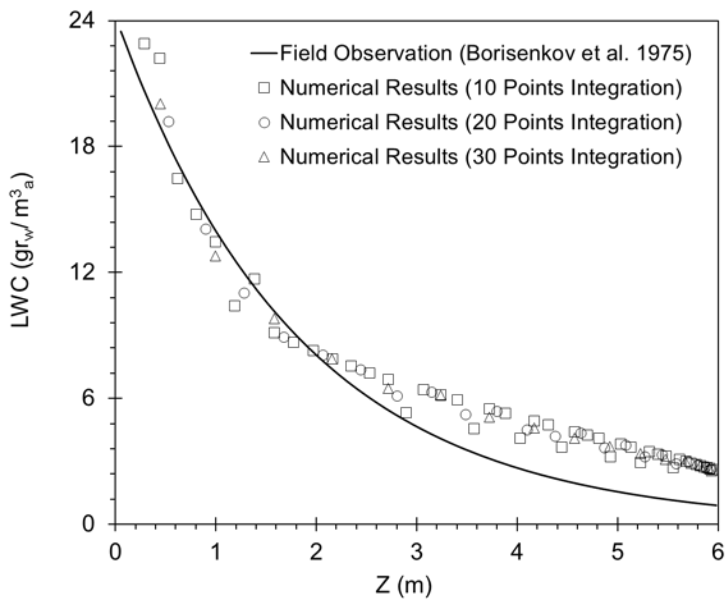

Fig. 13. Comparison between numerical results and field observations